

Consumption of a multi-deficient diet causes dynamic changes in the intestinal morphofunctional barrier, body composition and impaired physical development in post-weaning mice

Samilly Albuquerque Ribeiro^{1*}, Francisco Adelvane de Paula Rodrigues¹, Marco Antonio de Freitas Clementino¹, Herlice do Nascimento Veras¹, Rômmulo Celly Lima Siqueira¹, Pedro Henrique Quintela Soares de Medeiros¹, Jeanine Moraes Pereira¹, Márcio Flávio Araújo Guanabara Júnior¹, José Kleybson de Sousa¹, Ana Karolina Silva Santos¹, Armênio Aguiar dos Santos¹, Bruna Leal Lima Maciel², Alexandre Havt¹ and Aldo Ângelo Moreira Lima¹

¹Pharmacology Postgraduation Program, Department of Physiology and Pharmacology, Faculty of Medicine, Federal University of Ceará, Fortaleza, Brazil

²Nutrition Postgraduation Program and Department of Nutrition, Federal University of Rio Grande do Norte, Natal, Brazil

(Submitted 29 July 2021 – Final revision received 2 March 2022 – Accepted 11 April 2022 – First published online 29 April 2022)

Abstract

Few studies have focused on nutrient-deficient diets and associated pathobiological dynamics of body composition and intestinal barrier function. This study evaluated the impact of a nutrient-deficient diet on physical development and intestinal morphofunctional barrier in mice. C57BL/6 (21 days of age) mice were fed a Northeastern Brazil regional basic diet (RBD) or a control diet for 21 d. The animals were subjected to bioimpedance analysis, lactulose test, morphometric analysis and quantitative reverse transcription-PCR to evaluate tight junctions and intestinal transporters. RBD feeding significantly reduced weight ($P < 0.05$) from day 5, weight gain from day 3 and tail length from day 14. The intake of RBD reduced total body water, extracellular fluid, fat mass and fat-free mass from day 7 ($P < 0.05$). RBD induced changes in the jejunum, with an increase in the villus:crypt ratio on day 7, followed by reduction on days 14 and 21 ($P < 0.05$). Lactulose:mannitol ratio increased on day 14 ($P < 0.05$). Changes in intestinal barrier function on day 14 were associated with reductions in claudin-1 and occludin, and on day 21, there was a reduction in the levels of claudin-2 and occludin. SGLT-1 levels decreased on day 21. RBD compromises body composition and physical development with dynamic changes in intestinal barrier morphofunctional. RBD is associated with damage to intestinal permeability, reduced levels of claudin-1 and occludin transcripts and return of bowel function in a chronic period.

Key words: Malnutrition: Northeastern Brazil regional basic diet: Intestinal barrier function: Body composition: Tight junction proteins

Malnutrition is a serious public health problem, especially in developing countries⁽¹⁾. In 2020, approximately 149.2 million children under 5 years of age were affected by stunting, and approximately 45.4 million children under 5 years of age were affected by wasting⁽¹⁾. The WHO has indicated a reduction in rates of both in recent years; however, it is estimated that the economic crisis caused by pandemic COVID-19 increased the number of children affected by wasting by 15 % and is expected to increase the number of children affected by stunting in the coming years⁽²⁾. Nutritional deficiency, especially in the first years of life, is associated with impairment of the immune system⁽³⁾, increased susceptibility to infectious diseases⁽⁴⁾, growth

development⁽⁵⁾, cognitive deficit⁽⁶⁾ and increased susceptibility to chronic diseases in adulthood⁽⁷⁾, such as type II diabetes, CVD, obesity, hypertension and dyslipidaemia.

Animal models provide a better understanding of the pathophysiology associated with malnutrition. Different types of diets with nutritional deficiency have been evaluated for malnutrition in animal models^(7–10), including the Northeastern Brazil regional basic diet (RBD). RBD is a diet deficient in nutrients that mimics the dietary deficiencies of populations with low socio-economic status in the Brazilian semi-arid region⁽¹¹⁾. Since the first publication of the RBD, the diet has been explored to better understand the impact of acute or chronic malnutrition on the gastrointestinal

Abbreviations: RBD, regional basic diet.

* **Corresponding author:** Samilly Albuquerque Ribeiro, email samilly.ribeiro@hotmail.com

tract^(12,13), the transmission of maternal–fetal malnutrition⁽¹²⁾, the development of environmental enteropathy⁽¹⁴⁾ and the induction of the vicious cycle of enteric infection and malnutrition⁽¹⁵⁾, among others^(16–18).

The intestinal morphofunctional barrier is the largest surface area of the body and has vital life-maintaining functions, such as digestion, secretion, absorption of nutrients, electrolytes and water and defense function, recognition of microflora, food and toxin antigens⁽¹⁹⁾. Insufficient energy consumption leads the body to important physiological changes for maintaining the function of vital organs⁽²⁰⁾. The intestinal mucosa has a high capacity for self-renewal and is quickly affected by malnutrition⁽²¹⁾. In this context, a better understanding of the intestinal morphofunctional dynamics in malnutrition is extremely important for the development of effective treatments. Thus, the present study aimed to assess the temporal impact of RBD consumption in the post-weaning period on body composition, morphology and intestinal barrier function.

Methods

Animals, diet and experimental design

C57BL/6 male mice (21 days old) were obtained from the Animal Industry Sector of the Department of Physiology and Pharmacology of the Federal University of Ceará. The mice (total of fifty-six) were maintained in boxes with wood shaving under the following conditions: temperature of 22 (SEM 2°C), humidity of 60 (SEM 5) %, light/dark cycle of 12/12 h and free access to food and water. All procedures were conducted in accordance with the guidelines of the National Council for the Control of Animal Experimentation and approved by the Ethics Committee on the Use of Animals of the Federal University of Ceará (protocol 17/15).

Mice were randomly distributed in the nourished and malnourished groups (n 6 for group). Malnutrition was induced by the consumption of RBD (malnourished group), while healthy status was induced by the consumption of the control diet (nourished group). The RBD and control isoenergetic diets were purchased from the company Rhostrer® (Araçoiaba da Serra), and the composition of the diets is shown in **Table 1**. The animals were evaluated on day 0 and every two subsequent days for body weight and food and water consumption. Tail length was measured on day 0 and every 7 d after. On days 7, 14 and 21, the mice were subjected to body evaluation using electrical bioimpedance (ImpediVET® device), and the small intestine samples were collected for morphometric analysis and of the genes of intestinal transporters and tight junctions. Jejunum and ileum samples were collected after intramuscular anaesthesia with 90 mg/kg of ketamine and 10 mg/kg of xylazine and stored at –80°C or 10 % formaldehyde, and the animals were euthanised by exsanguination. The mice were also subjected to the lactulose and mannitol test protocols to analyse intestinal barrier function.

Measurement of body development

Tail length measurement is a parameter used in preclinical studies to estimate animal development in a non-invasive manner⁽¹⁴⁾.

Table 1. Composition of the regional basic diet and the control diet (Percentages)

	Control diet		RBD	
	%	%kcal	%	%kcal
Energy, kcal/g	3.7	–	3.7	–
Macronutrients				
Carbohydrates	58.21	63.41	73.47	83.94
Lipids	6.08	14.90	2.42	6.22
Protein	19.91	21.69	8.61	9.84
Fibre	3.7	–	2.94	–
Micronutrients				
Minerals	3.8	–	2.65	–
Total		100		100
Ingredient	%		%	
Maize starch	27.829		49.91	
Casein	23.151		6.36	
Dextrinized starch	4.202		6.27	
Dextrose or D-glucose anhydrous	23.343		22.40	
Inulin	2.334		2.24	
Sucrose	0.00		0.49	
Soya oil	6.536		2.09	
Cellulose MC-101	7.003		6.72	
Mineral mix Ca P K (RH9531UI)	0.934		0.45	
Bibasic calcium phosphate	1.214		0.99	
Calcium carbonate	0.514		0.00	
Potassium citrate	1.541		0.73	
Vitamin mix AIN-76 (RH9505UI)	0.934		0.90	
L-Cystine	0.280		0.10	
Sodium chloride	0		0.17	
Choline bitartrate	0.187		0.18	
Total	100		100	

The mice were positioned on a surface, the tail was extended distally and straight and the tail was measured from base to tip using a digital calliper (Mitutoyo® Precision Measuring Tools). The measurements were performed on days 0, 7, 14 and 21.

Electrical bioimpedance

After anaesthesia, the animals were placed on a non-conductive surface with posterior and anterior limbs extended perpendicular to the body, and the tail was extended distally. Four needles (25 × 12 gauge) were used as electrodes, inserted in the sub-dermal region along the dorsal midline. The central electrodes were inserted in the medial region between the ears and at the base of the tail, intercepting the imaginary line of the thigh muscle with the midline of the body. Peripheral electrodes were inserted between the eyes, approximately 1.0 cm from the electrode between the ears, and in the tail, approximately 1.0 cm of the electrode at the base of the tail. The needles were then attached to the ImpediVET® device, a single-channel tetra polar bioimpedance spectroscopy device that scans 256 frequencies between 4 and 1000 kHz in less than a second. The species, sex, age, length between central electrodes and body weight information were input to the equipment. An electric current was activated, and the resistance and reactance bioimpedance parameters were obtained from a single spectrum from 4 to 1 MHz in a series of 256 points. The device uses a complex impedance plot to determine total body water, extracellular fluid and intracellular fluid. The fat-free mass, fat mass and BMI were calculated using software coupled to the device, which uses values predefined for mice by the manufacturer⁽²²⁾.

Intestinal morphometry

Samples of the jejunum and ileum were sectioned longitudinally and fixed in 10% formaldehyde buffer for 18 h. After the fixation period, the material was dehydrated, embedded in paraffin, cut to 5.0 µm sections using an impact microtome (Polycut S) and stained with haematoxylin and eosin. Subsequently, with the aid of an optical microscope coupled to the image acquisition system (LEICA) and ImageJ software version 1.5a (National Institutes of Health), the heights of ten villi and the depths of ten crypts of each cut were measured to calculate the villus:crypt ratio.

Lactulose/mannitol test for intestinal barrier function studies in vivo

For sample collection, animals from both groups were kept in metabolic cages for a period of 24 h with an isoenergetic low-carbohydrate diet (Rhostrer®) before days 7, 14 and 21, 16 h corresponding to the period of adaptation to the collection environment and 8 h of fasting. We conducted experimental groups only for this test, so that the 8-h fasting would not interfere with other analyses. After fasting, all animals received 250 µl of the test solution by gavage, containing 5.0 g of lactulose (Duphar Laboratories) and 1.0 g of mannitol (Henrifarma Chemicals and Pharmaceuticals LTDA) dissolved in 20 ml of water. Urine samples preserved in 0.236 mg/ml chlorhexidine (Sigma Chemical®) were collected 24 h after the test solution was administered. The volumes of the samples were registered and centrifuged at 10 000 rpm for 3 min, and then 50 µl of a solution of the internal standard (3.6 mM of melibiosid diluted in 2.9 ml of distilled water) was added to 50 µl of each sample. The solution was deionised and centrifuged (10 000 rpm for 3 min), and 50 µl was used to determine sugar by high-pressure liquid chromatography on an UltiMate 3000 instrument (Thermo Fisher Scientific®). Two standard carbohydrate solutions were used to calibrate the system at the beginning and between the testing of each group. The standards contained 60 µM of sugars: glucosamine, mannitol, melibiose and lactulose (group I) and inositol, sorbitol, glucose and lactose (group II). Groups I and II were applied at a concentration of 0.1 mM to determine the intra-experiment variation. The concentrations of lactulose and mannitol were measured for all experimental groups using high-pressure liquid chromatography with pulsed amperometric detection, as previously described⁽²³⁾.

Evaluation of gene transcription of tight junctions and intestinal transporter proteins

Gene transcription of the zonula occludens-1 (ZO-1), occludin, claudin-1 (CLAU-1), claudin-2 (CLAU-2), peptide transport 1 (PEPT-1) and SGLT-1 was determined by quantitative reverse transcription-PCR. The reference gene for normalisation was 18S. RNA extraction from total jejunum samples on days 7, 14 and 21 was performed according to the RNeasy Lipid Tissue Mini Kit protocol (Qiagen®). Then, 1 µg of the total isolated RNA was used for cDNA synthesis using the iScript cDNA Synthesis Kit (Bio-Rad®), according to the manufacturer's instructions. For the reaction, 10 µl of Syber Green PCR Master Mix (Applied Biosystems), 2.0 µl of each primer (0.2 µM) and

1.0 µl of cDNA from samples were used, and nuclease-free water was added to an end volume of 20 µl. The sequences and annealing conditions obtained from the National Center for Biotechnology Information website for each investigated gene are listed in Table 2. The data obtained were based on the values of the threshold cycle, in which the observed fluorescence was ten times greater than the baseline fluorescence for each qPCR assay. All amplifications were evaluated for the melting curve and performed to ensure the specificity of the amplification and to detect the formation of initiator dimers or any other non-specific product. From the values of the quantitative cycle (Cq/Ct), the relative levels of RNA were calculated according to the $2^{-\Delta\Delta Ct}$ method⁽²⁴⁾.

Evaluation of relative protein expression of tight junctions and intestinal transporter proteins

The investigation of protein expression of tight junctions and transporters involved in the regulation of the intestinal barrier was carried out using western blotting. The jejuna isolated from the animals were homogenised in RIPA buffer (Thermo Fisher Scientific®) with protease inhibitor (1 ml inhibitor: 100 ml RIPA) and centrifuged at 10 000 rpm for 10 min. The total amount of protein in each sample was measured using the Pierce™ BCA protein assay kit (Thermo Fisher Scientific®). Samples (120 µg of protein) were prepared by adding Laemmli buffer (Bio-Rad) with β-mercaptoethanol (Bio-Rad®), denatured at 99°C for 5 min. Proteins were separated by SDS-PAGE (8–10% for SGLT-1, PEPT-1 and occludin; 15% for claudin-1 and -2), transferred to polyvinylidene difluoride membrane, blocked with 5% bovine serum albumin for 1 h and incubated with primary rabbit antibody: anti-GAPDH (1:1000), anti-SGLT-1 (1:500), anti-PEPT-1 (1:200), anti-occludin (1:1000), anti-claudin-1 (1:200) and anti-claudin-2 (1:200) (Santa Cruz Biotechnology®). The membranes were also incubated for 1.5 h with the secondary antibody and then developed using the Clarity Western ECL Substrate kit (Bio-Rad®) and the ChemiDoc system (Bio-Rad). The densitometric quantification of the bands was analysed using ImageLab 6.0 software (Bio-Rad®).

Statistical analysis

Parametric data were analysed by Student's *t* test or ANOVA followed by the Bonferroni post-test for paired data. Non-parametric data were analysed using the *Mann-Whitney* test. The parametric results are presented as mean values with their standard error of the mean, and the non-parametric results are presented as median and minimum to maximum. All tests were analysed using GraphPad Prism® software, and the results were considered significant at $P < 0.05$.

Results

Regional basic diet effect in body composition and development of weanling mice

The consumption of RBD caused a significant reduction ($P < 0.001$) in the weights of malnourished animals from day 5 to day 21 when compared with the nourished animals (Fig. 1(a)). Weight gain



Table 2. Genes, primers, accession number and conditions of quantitative reverse transcription -PCR

Genes	Primer sequence (5'-3')	NCBI no.	Annealing conditions*
<i>Claudin-1</i>	TCTACGAGGGACTGTGGATG TCAGATTCAGCAAGGAGTCG	NM_016674-4	20', 58°C
<i>Claudin-2</i>	CCCACCACCACAGCTTAAT GAAATGGCTTCCAGGTCAGC	NM_016675-4	20', 60°C
<i>Occludin</i>	AAGAGCAGCCAAAGGCTTCC CGTCGGGTTCCTCCCATTA	NM_008756-2	20', 60°C
<i>ZO-1</i>	GACCATCGCCTACGGTTTGA AGGTCTCGGGGATGCTGATT	NM_001163574-1	20', 60°C
<i>SGLT-1</i>	CGGAAGAAGCGATCTGAGAA AATCAGCACGAGGATGAACA	NM_019810-4	20', 58°C
<i>PepT-1</i>	AGGGGAGAACGGAATCAGGT CTTTTCGCCAGAAGGGAAGA	NM_053079-2	20', 60 °C
<i>18S</i>	AATGCTGGACCAAACACAAA TTCCACAATGTTTCATGCCTT	NM_008907-1	20', 58°C

* Total of forty cycles, all cycles started with the denaturation stage (20 s at 95°C) and ended with an extension stage (45 s for 1 min at 72°C).

decreased significantly ($P < 0.001$) in the malnourished group from day 3 when compared with the malnourished group (Fig. 1(b)). Malnourished animals increased their weight and significantly gained weight over time ($P < 0.001$), in which weight increased from day 7 and weight gain increased from day 9 when compared with the values measured on day 0 (Fig. 1(a) and (b)). Tail length was significantly shorter ($P < 0.05$) in the malnourished group than in the nourished group on days 14 and 21 (Fig. 1(c)). Chronic consumption of the RBD diet compromised the animals' body development (Fig. 1(d)) regardless of feed consumption because there was a significant difference ($P < 0.05$) in the consumption between the groups only on day 3 (Fig. 1(e)). The malnourished group consumed 18.55% less feed than the nourished group only on day 3 (nourished 3.45 (SEM 0.08) *v.* malnourished 2.81 (SEM 0.15) g), whereas water consumption was 31.19% higher in the malnourished group than in the control group only on day 21 (nourished 7.5 (SEM 0.5) *v.* malnourished 10.9 (SEM 0.6) ml, $P < 0.05$, Fig. 1(f)).

Considering the body composition of the animals, total body water significantly reduced ($P < 0.05$) in the malnourished group compared with the nourished group from day 7 (Fig. 2(a)). The extracellular fluid significantly reduced ($P < 0.05$) in the malnourished group compared with the nourished group on days 7, 14 and 21 (Fig. 2(b)). In contrast, intracellular fluid significantly reduced in the malnourished group when compared with the nourished group on days 7 (nourished 3.15 (SEM 0.22) *v.* malnourished 1.88 (SEM 0.25) ml, $P < 0.01$) and 14 (nourished 3.85 (SEM 0.16) *v.* malnourished 2.81 (SEM 0.33) ml, $P < 0.05$, Fig. 2(c)). In addition, the RBD diet caused a significant reduction ($P < 0.01$, $P < 0.05$) in the fat-free mass (Fig. 2(d)) and fat mass (Fig. 2(e)) on days 7, 14 and 21 when compared with those of the nourished group. However, the BMI did not change at any of the analysed time points (Fig. 2(f)).

Temporal effect of regional basic diet consumption on intestinal morphology

RBD intake dynamically altered the morphometry of the portions of the jejunum (Fig. 3) and ileum (Fig. 4) over time. A significant reduction ($P < 0.01$) in the crypt depth and a significant increase ($P < 0.05$) in the villus:crypt ratio in the jejunum of malnourished animals were observed on day 7. No significant changes were

observed in the ileum on day 7. On the other hand, on the 14th day the villus:crypt ratio significantly reduced ($P < 0.05$) in the jejunum of malnourished animals (Fig. 3(c)), without significant changes in villus height and crypt depths, while in the ileum a significant reduction was observed ($P < 0.001$) at the height of the villi of the malnourished animals (Fig. 4(a)). On day 21, there was a significant reduction ($P < 0.05$) in the height of the villi (Fig. 3(a)) and maintenance in the reduction of the villus:crypt ratio in the jejunum of malnourished animals (Fig. 3(c)), without significant changes in the ileal portion (Fig. 4(c)).

Temporal effect of regional basic diet consumption on intestinal barrier function

RBD also caused time-dependent changes in intestinal permeability. When assessing the percentage of lactulose excretion, it was possible to observe a significant reduction ($P < 0.01$, $P < 0.05$) in the malnourished group compared with the nourished group on days 7 and 14 (Fig. 5(a)). The percentage of mannitol excretion was also significantly reduced ($P < 0.05$) in malnourished animals when compared with that observed on days 7 and 14 (Fig. 5(b)). The lactulose:mannitol ratio increased significantly ($P < 0.05$) in malnourished animals compared with that in animals fed on day 14 (Fig. 5(c)). No significant changes in intestinal barrier function were observed on day 21.

Temporal effect of regional basic diet consumption on the relative transcription of tight junctions and intestinal transporters

Analysis of the relative infrastructure of protein-forming proteins in the jejunum allowed us to assess the dynamics of changes in the molecular architecture of the intestinal barrier. The relative transcription of clau-1 was significantly reduced ($P < 0.05$) in the malnourished group compared with the nourished group on day 14 (Fig. 6(a)), whereas Clau-2 was significantly reduced in the malnourished group compared with the nourished group on day 21 (Fig. 6(b)). The relative transcription of occludin was significantly reduced ($P < 0.05$) in the malnourished group compared with that in the nourished group on

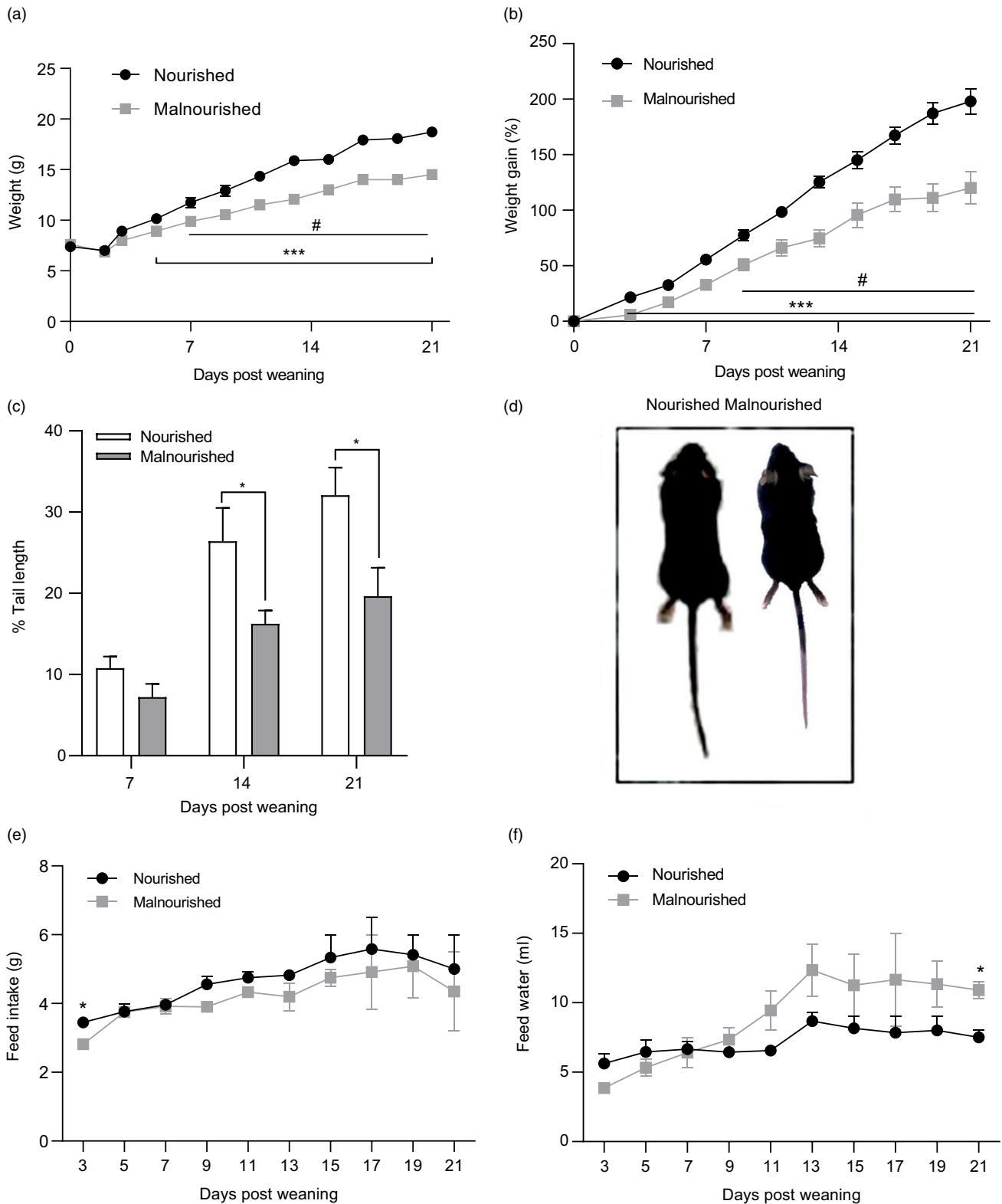


Fig. 1. Growth rate in weaning mice fed for regional basic diet or control diet. (a) Weight and (b) weight gain of C57BL/6 nourished and malnourished animals for a total of 21 d after weaning. The data are representative of three different experiments ($n=6-8$ per group). Weight and weight gain were measured every 2 days and the data are presented as mean values with their standard error of the mean ($***P < 0.001$, Student's t test nourished v. malnourished per day and $\# P < 0.001$ ANOVA of repeated measures comparing the days of the malnourished group with day 0). (c) Tail length variation of nourished (white bar) and malnourished (grey bar) animals on days 7, 14 and 21 ($n=6-8$ per group). The data represent the percentage of tail length variation in mean values with their standard error of the mean ($*P < 0.05$, Student's t test nourished v. malnourished by time). (d) Representative image of the global effects of nourished and malnourished animals on day 21. (e) Feed and water (f) consumption during the 21 experimental days ($n=6-8$ per group). The data represent the mean consumption of each group ($n=6-8$ mice per group) in three different experiments. Data are presented as mean values with their standard error of the mean ($*P < 0.05$, Student's t test, nourished v. malnourished per day).

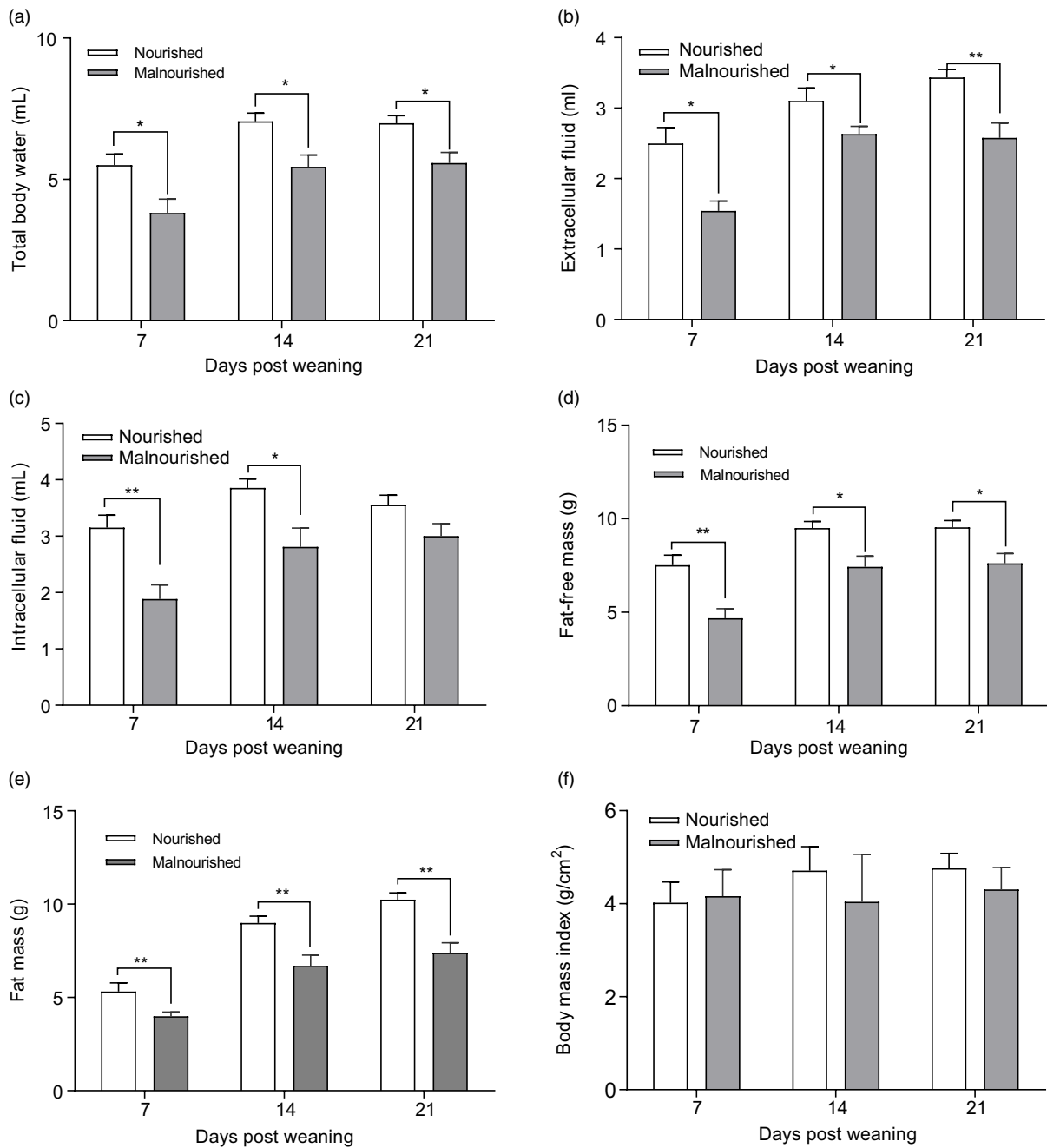


Fig. 2. Body composition of animals submitted to the consumption of regional basic diet (RBD) or control diet. After challenging the animals with RBD diet and control diet ($n=8$), we analysed on days 7, 14 and 21 (a) total body water, (b) extracellular fluid, (c) intracellular fluid, (d) fat-free mass, (e) fat mass and (f) BMI. The data for each time represent different experimental lines and the data are presented by mean values with their standard error of the mean (* $P < 0.05$, ** $P < 0.01$, nourished v. malnourished, Student's t test).

days 14 and 21 (Fig. 6(c)). In contrast, the relative transcription of ZO-1 was not altered at any time point analysed (Fig. 6(d)).

The consumption of RBD also altered the analysis of the relative transcription of intestinal transporters. The relative transcription of PEPT-1 increased significantly ($P < 0.05$) in the malnourished group compared with the nourished group only on day 7 (Fig. 6(e)). The SGLT-1 levels increased significantly on days 7 and 14 in the malnourished group when compared with the nourished group; however, the GLUT decreased

significantly on day 21 in the malnourished group when compared with the nourished group (Fig. 6(f)).

Temporal effect of regional basic diet consumption on the relative protein expression of tight junctions and intestinal transporters

The evaluation of the relative protein expression of tight junctions and intestinal transporters allowed us to identify those

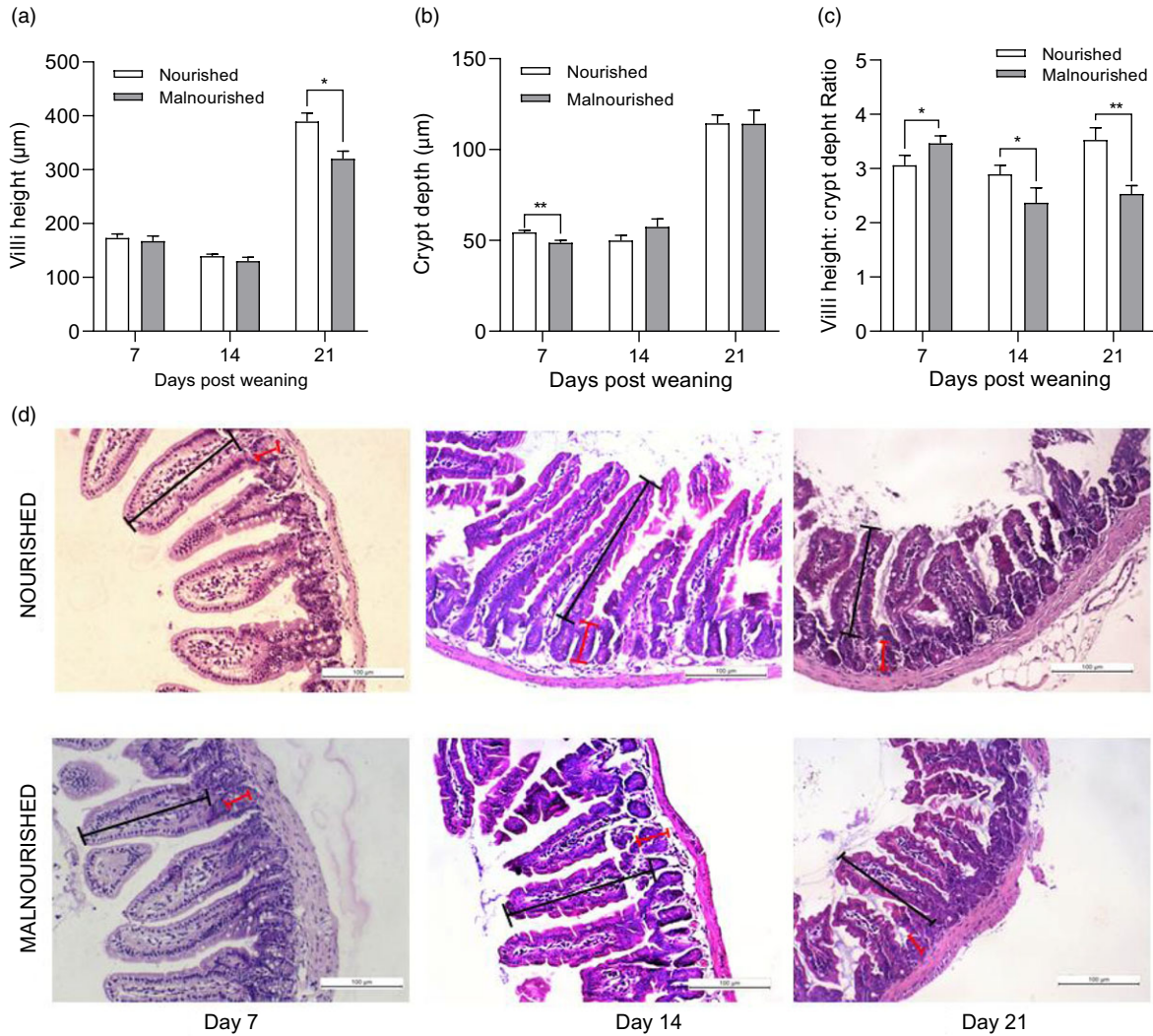


Fig. 3. Jejunum morphometry of nourished or malnourished animals. (a) Villus height (black line), (b) crypt depths (red line) and (c) villus height: crypt depth ratio were recorded for the nourished (white bar) and malnourished (grey bar) group on days 7, 14 and 21 ($n4$). Data are presented as mean values with their standard error of the mean (* $P < 0.05$, ** $P < 0.01$, Mann Whitney test on nutrient v. malnutrition for each day). (D) Sections of the nourished and malnourished mice stained with the haematoxylin and eosin standard for all times.

alterations found for relative transcription were not the same for protein expression. On day 7, we observed a trend towards increased protein expression of SGLT-1 and PepT-1 in malnourished animals compared with nourished ones, but with no significant difference ($P > 0.05$) (Fig. 7(a)). On day 14, the relative protein expression of SGLT-1 and occludin showed a trend ($P > 0.05$) to increase in malnourished animals when compared with nourished animals (Fig. 7(b)). Regarding day 21, we observed a certain trend ($P > 0.05$) towards increased protein expression of SGLT-1, Clau-2 and occludin in the malnourished group when compared with the control group (Fig. 7(c)).

Discussion

In this study, the ingestion of RBD triggered atrophy in body development; compromised body composition; and affected intestinal morphological histology, intestinal barrier function

and mRNA levels of tight junctions and intestinal transporters, which are essential proteins for maintaining the morphofunctional barrier and adequate nutrient absorption, respectively

Nutritional deficiency during early childhood is directly related to short- and long-term consequences resulting from adaptive epigenetic responses⁽²⁵⁾. In this context, the development of weanling animal models has helped to better understand the pathophysiology associated with multi-deficient diets^(9,25,26). Our results, which differed from those of studies reported in the literature, allowed a temporal assessment of changes triggered by a diet exhibiting multiple nutrient deficiencies, based on food composition intake in the Northeastern Brazil, in the body composition, intestinal morphology and barrier function, and physical development of weanling rodents.

RBD is an experimental diet low in lipids, proteins and minerals and rich in carbohydrates, which is characteristic of diets accessible to low-income populations in Northeastern Brazil⁽¹¹⁾.

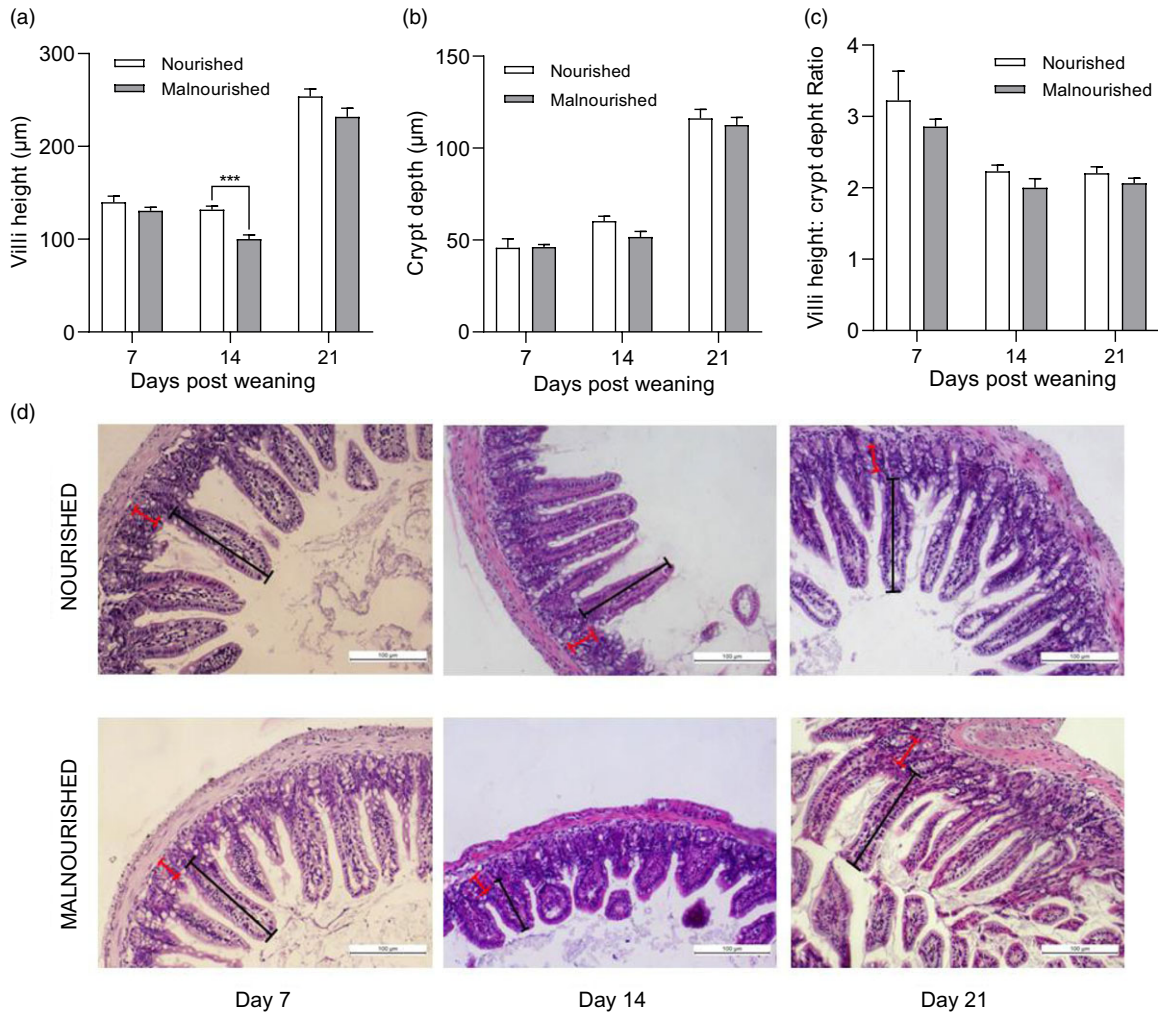


Fig. 4. Morphometry of the ileum of nourished or malnourished animals. (a) Villus height (black line), (b) crypt depths (red line) and (c) villus height/crypt depth ratio were recorded for the nourished (white bar) and malnourished (grey bar) group on days 7, 14 and 21 (n 4). Data are presented as mean values with their standard error of the mean ($***P < 0.001$, Mann Whitney test on nutrient v. malnutrition for each day). (d) Sections of the nourished and malnourished mice stained with the haematoxylin and eosin standard for all times.

RBD-induced malnutrition in weanling mice is characterised by rapid weight reduction and weight gain^(12–14) and a late reduction in tail length⁽¹⁴⁾. Our results show that RBD reduces weight gain early, followed by a reduction in weight in the first week and impaired growth from the second week of consumption of RBD, without changes in BMI due to both weight and length deficits. Our results were similar to the literature, even with our RBD lipid values being higher than in other studies^(11,12,27). In the literature, we have observed a variation of 0.8%^(11,12,27) to 8.2%⁽¹³⁾ of fat, in this sense our study maintained a percentage of 6.2% kcal of fat, thus within this percentage variation. In addition, changes in weight, weight gain and tail length occurred without changes in diet consumption, probably because diets were isoenergetic. Most studies with nutrient-deficient and isoenergetic diets do not report food consumption in the groups^(12,14–16), except for Sampaio *et al.*⁽¹³⁾ who observed differences in feed intake on day 2.

The consumption of RBD in this study led to reduced total body water, extracellular fluid, fat mass and fat-free mass from day 7, while intracellular fluid decreased on days 7 and 14.

Bioelectrical impedance is rarely considered in animal studies, and to date, no study has analysed the body composition of animals in nutritional deficiency models. However, it is known that the metabolism of several organs in malnutrition is sustained by the mobilisation of fat and protein reserves when protein consumption is insufficient to maintain protein metabolism⁽²⁸⁾. Therefore, our results show that the nutritional deficiency of the RBD diet is capable of compromising the animals' body energy reserves. In addition, the absence of oedema occurred even as increased water consumption in malnourished animals. In the clinic, severe acute malnutrition may present with the presence or absence of oedema⁽²⁹⁾. Studies indicate that a low-protein diet decreases urine concentration capacity and free water reabsorption in the kidney due to synergistic or contributory changes, such as reduced corticomedullary osmotic gradient, reduced plasma amino acids, hydrosmotic effect of decreased ADH, among others⁽³⁰⁾. Therefore, a possible change in water reabsorption in the kidney triggered by protein deficiency in RBD may explain the increase in water consumption and absence of oedema in the present study.

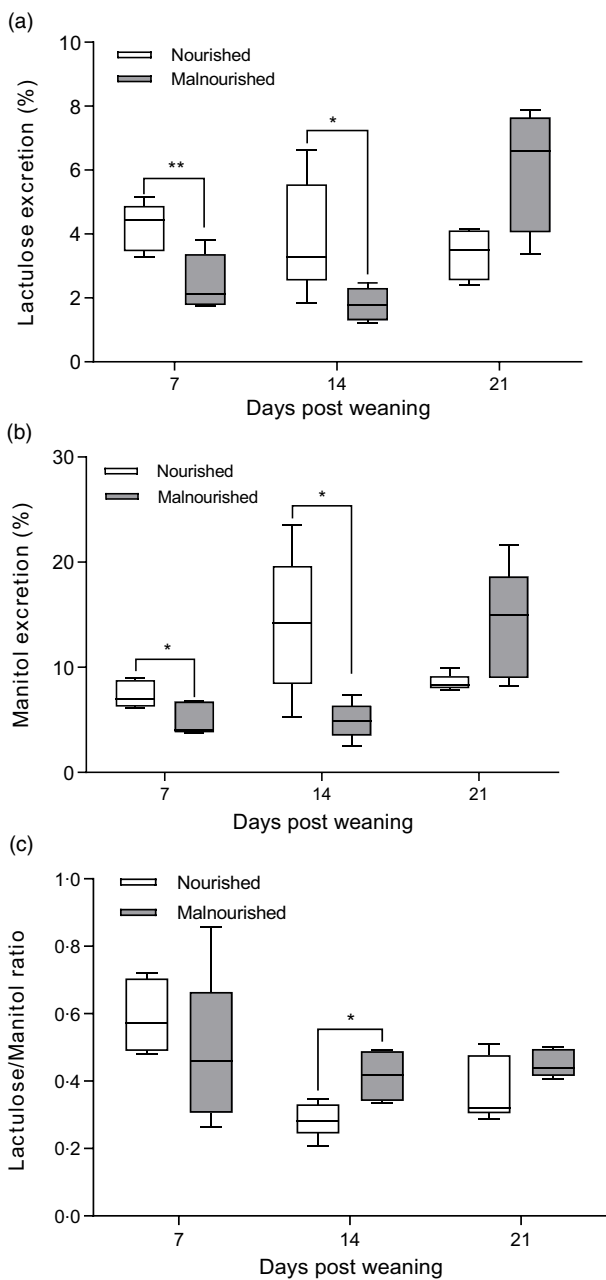


Fig. 5. Effects of RBD consumption on intestinal permeability on days 7, 14 and 21. The percentage excretion of (a) lactulose, (b) mannitol and (c) lactulose/mannitol ratio was recorded on days 7, 14 and 21 in the nourished and malnourished groups. The data correspond to an experiment (n 6). Data are presented as median and minimum to maximum for all times (* P < 0.05, ** P < 0.01, Mann-Whitney test by time).

Differentiation of intracellular and extracellular fluids is important for nutritional assessment⁽³¹⁾. Chronic malnutrition is reported to compromise the growth of intracellular fluids and induce increases in extracellular fluids over time⁽³²⁾. However, in this study, RBD caused atrophy of extracellular fluid from early to chronic, while intracellular fluid atrophied on days 7 and 14, with a return to baseline in a more chronic period. Intracellular fluid provides a baseline for measuring oxygen consumption, energetic requirements and BMR, while extracellular fluid

indicates most collagen-derived tissues, as well as interstitial fluid and plasma⁽³³⁾. Cheek *et al.*⁽³⁴⁾ reported that the restoration of the cell phase or metabolically active protoplasm is of great importance for maintaining metabolism. Therefore, the return of intracellular fluid to the basal state indicates restoration of the metabolic rate on the 21st day.

The gastrointestinal tract is the first system directly affected by changes in nutrient intake, exhibiting rapid physiological and morphological changes⁽³⁵⁾. In this study, RBD also triggered adaptive responses in intestinal barrier function. In a short time, RBD triggered atrophy of crypts and an increased villus: crypt ratio of the jejunum without altering the morphology of the ileum. Then, the RBD atrophied the absorptive area of the jejunum and reduced the height of villi in the ileum; and, in a chronic period, the RBD reduced the height of villi and the absorptive area in the jejunum. The morphological changes observed in this study are different from those reported in the literature; however, no work to date has evaluated the temporal effect of the RBD diet on the intestinal morphofunctional barrier. A study similar to ours showed that RBD-induced malnutrition reduces the height of the ileal crypt in a short period⁽¹³⁾. On the other hand, a model of RBD-induced malnutrition caused villus dullness, promoted crypt depth and decreased the villus: crypt ratio in the jejunum at 14 d⁽¹⁶⁾. However, another study showed that malnutrition in weanling mice due to a diet similar to RBD caused no morphological changes in any portion of the intestine analysed after 21 d⁽¹⁴⁾. The intestinal barrier is highly dynamic and changes easily⁽³⁶⁾. Therefore, our results show an increase in the absorptive area in the initial phase that is not sustained in a later period, likely due to RBD protein deficiency.

In clinical settings, malnourished children exhibit greater intestinal permeability^(37,38). Experimental models, mainly models of chronic malnutrition, also indicate damage to the intestinal cell barrier^(12,14). In this context, the lactulose and mannitol test (L/M) is a consistent, non-invasive and sensitive marker for intestinal barrier function^(39,40). In the present study, intestinal barrier function changed dynamically over time. RBD-induced malnutrition caused a reduction in the total absorptive area and paracellular permeability, with no indication of damage to the barrier on day 7. In contrast, day 14 showed a reduction in the absorptive area, increased paracellular permeability and consequent barrier damage that was reversed on day 21 in malnourished animals, consistent with restoration of the metabolic rate.

The L/M test is widely used in clinics to diagnose environmental enteropathy⁽⁴¹⁻⁴³⁾ and verify the effectiveness of treatments for malnutrition and diarrheal infections^(21,37,38). The moderate acute malnutrition-induced RBD did not alter transepithelial resistance during substrate absorption, indicating that in acute models, the diet does not affect paracellular permeability⁽¹³⁾, in contrast to the present study. A porcine model also identified that transepithelial resistance was not altered during acute malnutrition⁽⁴⁴⁾. No RBD-induced malnutrition model showed changes in intestinal permeability on day 14, but a model similar to ours, with weanling mice challenged with an RBD-like diet showed barrier damage on day 21⁽¹⁴⁾. Changes in intestinal barrier function on day 14 were concomitant with a reduction in cell mass, muscle mass and adipose tissue, indicating a

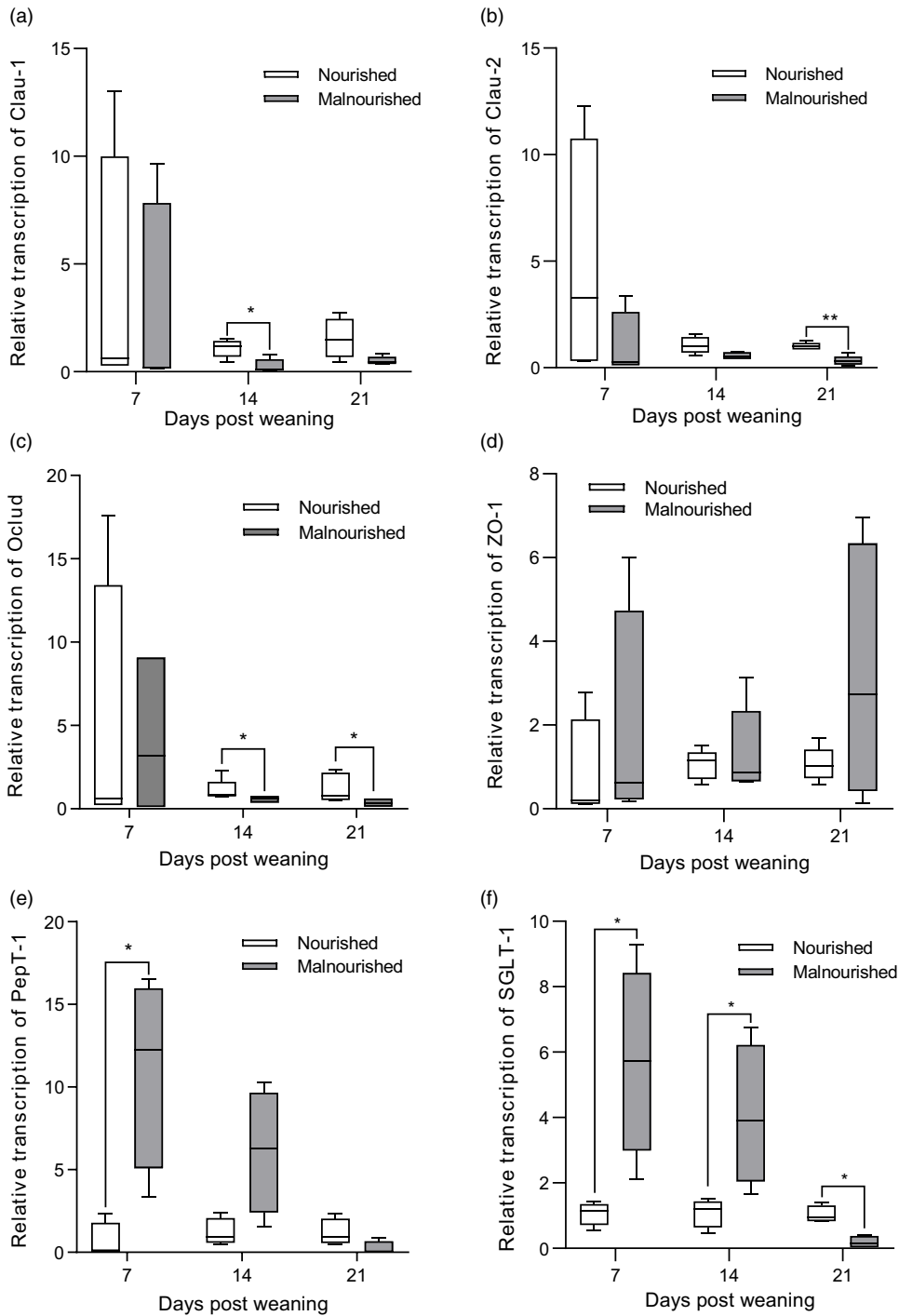


Fig. 6. Relative transcription of tight junctions and intestinal transporters in the jejunum of nourished and malnourished mice on days 7, 14 and 21. Analysis of the relative transcription of (a) claudin-1 (clau-1), (b) claudin-2 (Clau-2), (c) occludin (occlud), (d) ZO-1, (e) PepT-1 and (f) SGLT-1. Data are presented as median and minimum to maximum for all times (n 6, * $P < 0.05$, ** $P < 0.01$, Mann-Whitney test by time).

reduction in energy reserves necessary for repair response. The absence of changes in intestinal barrier function on day 21 may be due to the return of the metabolic rate, indicated by the absence of changes in intracellular fluids.

Several proteins constitute tight junctions and have complex distribution, regulation and functional characteristics^(45–47).

Overexpression of occludin in epithelial cells *in vitro* triggers an increase in transepithelial electrical resistance and an unexplained increase in the flow of uncharged solutes^(48,49). In contrast, claudin-1 plays a crucial role in barrier formation in several organs⁽⁴⁷⁾. Unlike claudin-2, which plays a role in pore function, is indispensable for Na^+ absorption in mice⁽⁴⁵⁾. Our

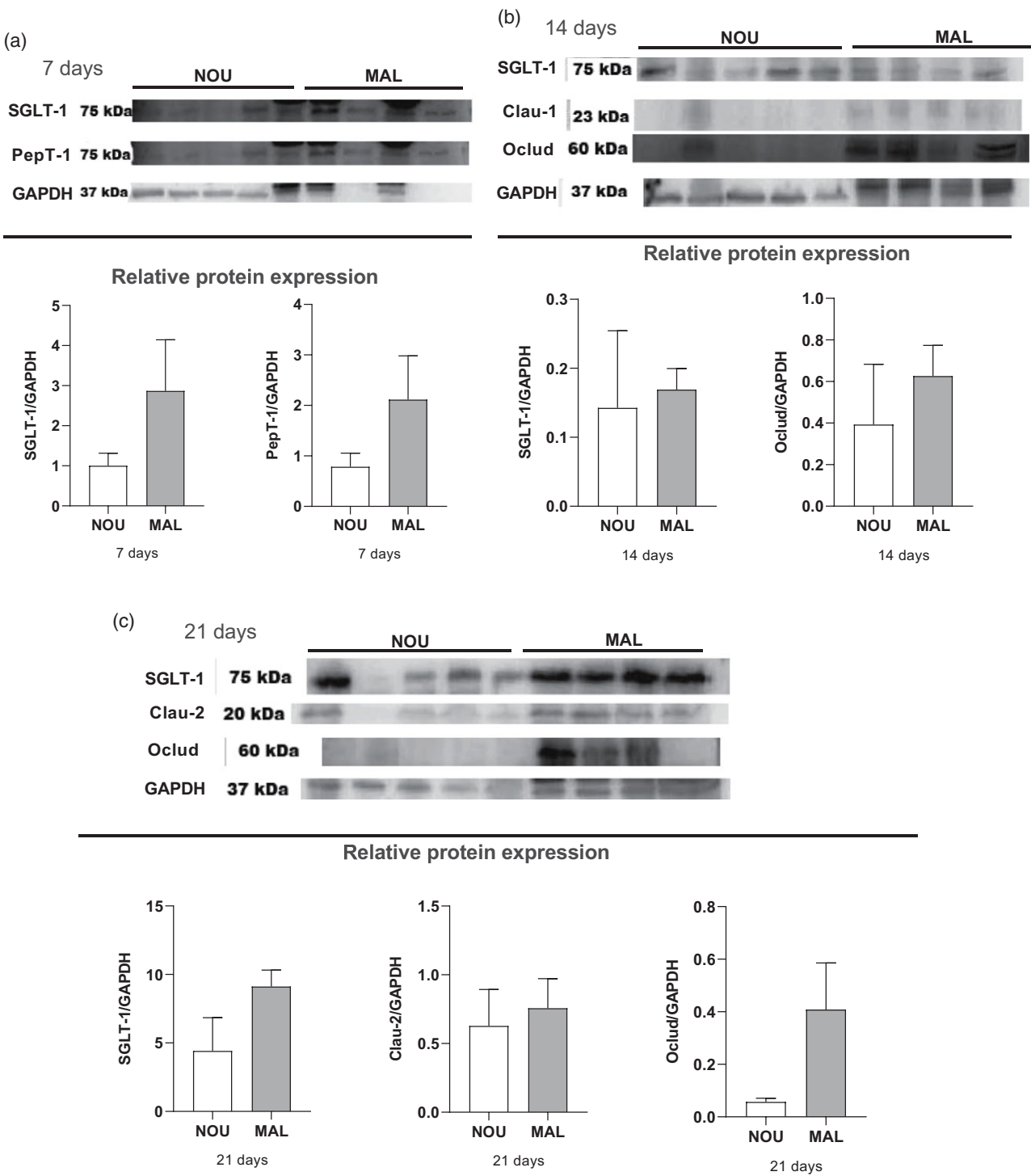


Fig. 7. Relative protein expression of tight junctions and intestinal transporters of nourished and malnourished mice on days 7, 14 and 21. (a) Representative western blot analysis of SGLT-1, PepT-1 and GAPDH on day 7 followed by quantitative results of relative protein levels. (b) Representative western blot analysis of SGLT-1, Clau-1 and Occludin and GAPDH on day 14 followed by quantitative results of relative protein levels. (c) Representative western blot analysis of SGLT-1, Clau-2 and Occludin and GAPDH on day 21 followed by quantitative results of relative protein levels. Data are presented as mean values with their standard error of the mean for all times ($n = 4-5$, Mann-Whitney test by time).

results showed that RBD did not stimulate any change in the levels of transcripts of tight junctions on the 7th day, but on the 14th triggered reduction in the levels of claudin-1 and occludin, and on day 21st levels of claudin-2 and occludin were reduced, no

significant changes in protein levels. Claudins are a family of twenty-seven proteins that are considered the most important constituents for the maintenance of intestinal epithelial barrier homeostasis⁽⁵⁰⁾. In the literature, different models of nutritional

deficiency consumption showed different modulations in transcript levels and the expression of firm junctions, but no work reported temporal changes in these proteins. For example, a model of moderate acute malnutrition with RBD in post-weaning mice showed increased levels of claudin-2 and occludin mRNA in the ileum, with no change in protein expression⁽¹³⁾. Post-weaning RBD-induced malnutrition results in a reduction in ZO-1 mRNA levels and an increase in claudin-2 levels during the chronic period⁽¹⁴⁾. RBD-induced malnutrition in neonates triggered an increase in the expression of claudin-3, but not claudin-1, occludin and ZO-1 expression⁽¹²⁾. In contrast, severe protein deprivation has been reported to decrease the protein expression of claudin-1, but with no change in the expression of occludin in the small intestines of neonatal rats⁽⁵¹⁾. Therefore, these data show that mRNA transcription and expression of tight junction proteins are highly dynamic, complex and dependent on various experimental and animal conditions.

Morphological and functional changes can promote beneficial or harmful effects on the transport of nutrients and ions, resulting from an adaptive mechanism to malnutrition⁽³⁵⁾. In the present study, RBD-induced malnutrition in PEPT-1 mRNA levels increased only on day 7, while SGLT-1 mRNA levels increased on days 7 and 14 and decreased on day 21, no changes in protein levels. The regulation of gene expression of intestinal transporters is complex and can be altered under different conditions⁽⁵³⁾. RBD induced an increase in the levels of SGLT-1 and PEPT-1 transcripts in the ileum on day 7, with no changes in protein expression⁽¹³⁾. The levels of SGLT-1 transporters are known to be highly correlated with the amount of food carbohydrates⁽⁵⁴⁾. Studies indicate that a diet rich in carbohydrates increases the expression and levels of SGLT-1 transcripts and consequently the absorption of glucose within 1–3 d^(54,55). However, low protein diets stimulate an increase in the expression of essential amino acid transporters, aiming at cost benefits^(35,56). Our data show an increase in the levels of transporter mRNA initially to maintain adequate nutrient absorption; however, energy deprivation over time does not allow these changes to be observed in protein expression and promotes the reduction of these transporter mRNA levels later.

The present study was limited by the lack of quantification of protein expression and levels of claudin-15 and GLUT transcripts together with the application of tests such as oral glucose tolerance and measurement of the blood amino acid profile would allow identification of changes in the intestinal absorption of nutrients, thus reinforcing the changes identified for transporters. In addition, functional tests such as Ussing chambers associated with transmission electron microscopy could better explain the electrophysiological changes and distribution of proteins forming firm junctions at the paracellular level triggered by RBD in the intestinal epithelial barrier. Supplementation with alanyl-glutamine or Zn could also be added as a possible treatment for the effects of RBD. However, the present work shows that the intestinal morphofunctional barrier can adapt positively to nutrient deprivation, probably with the aim of maintaining intestinal function. Thus, this research makes an important contribution to better understand the impact over time that a multi-deficient

diet can have on important organs, such as the gastrointestinal tract.

In conclusion, RBD delays weight gain and physical development, changes body composition over a short period and induces long-term compositional alteration. In addition, a diet deficient in nutrients triggers a dynamic response in the intestinal function and morphology of the jejunum, which is associated with changes in the transcript levels of firm junctions and intestinal transporters. In a short period, RBD decreases the depth of crypts and increases the villus/crypt ratio of the jejunum, decreasing the total absorptive area and paracellular permeability, with increased levels of transcripts from the PEPT-1 and SGLT-1 transporters and without changing the transcript levels of tight junctions. The greatest damage to the morphofunctional barrier occurs in the intermediate period, with the reduction in the villus/crypt ratio of the jejunum, height of the villi in the ileum, paracellular permeability and total absorptive area with indicative barrier damage, which is associated with reduced transcript levels of claudin-1 and occludin and increased levels of the SGLT-1 transporter. In late periods, the villus/crypt ratio of the jejunum remains reduced in malnutrition, with a reduction in villus height, with no changes in intestinal barrier function, but a reduction in the levels of claudin-2, occludin and SGLT-1 transcripts. Thus, the present study provided monitoring of the main body and morphofunctional changes resulting from the introduction of a diet deficient in nutrients in a critical phase of physical development, enabling a dynamic understanding of the acute and chronic effects resulting from malnutrition and suggesting adaptive mechanisms in late periods, mainly in terms of intestinal barrier function.

Acknowledgements

We thank all researchers involved in development, financial support agencies and Gerly Brito (Federal University of Ceará, Fortaleza, Brazil).

There is no conflict of interest related to this manuscript.

This study was supported by National Council for Scientific and Technological Development (CNPq; #303650/2013–3). CNPq had no role in the design, analysis or writing of this article.

The responsibilities of the authors were as follows: S. A. R., F. A. P. R., P. H. Q. de M. and A. A. M. L.: designed the research; S. A. R., F. A. P. R., M. A. C., H. N. V., R. C. L. S., J. M. P.; M. F. A. G. J. and A. H.: conducted the study; S. A. R., F. A. P. R., J. K. de S., A. K. S. dos S., A. A. dos S., B. L. L. M., A. H. and A. A. M. L.: analysed and interpreted data; S. A. R. and A. A. M. L.: wrote the paper and had final responsibility for the content; and all authors: read and approved the manuscript.

References

1. Das S, Hossain MZ & Nesa MK (2009) Levels and trends in child malnutrition in Bangladesh. *Asia-Pac Popul J* **24**, 51–78.
2. Headey D, Heidkamp R, Osendarp S, *et al.* (2020) Impacts of COVID-19 on childhood malnutrition and nutrition-related mortality. *Lancet* **396**, 519–521.



3. Attia S, Versloot CJ, Voskuil W, *et al.* (2016) Mortality in children with complicated severe acute malnutrition is related to intestinal and systemic inflammation: an observational. *Am J Clin Nutr* **104**, 1441–1449.
4. Moore SR, Lima AA, Conaway MR, *et al.* (2001) Early childhood diarrhoea and helminthiases associate with long-term linear growth faltering. *Int J Epidemiol* **30**, 1457–1464.
5. Guerrant RL, Bolick DT & Swann JR (2021) Modeling enteropathy or diarrhea with the top bacterial and protozoal pathogens: differential determinants of outcomes. *ACS Infect Dis* **7**, 1020–1031.
6. Galler JR, Bryce CP, Zichlin ML, *et al.* (2012) Infant malnutrition is associated with persisting attention deficits in middle adulthood. *J Nutr* **142**, 788–794.
7. Deboer MD, Lima AA, Oría RB, *et al.* (2013) Early childhood growth failure and the developmental origins of adult disease: do enteric infections and malnutrition increase risk for the metabolic syndrome? *Nutr Rev* **70**, 642–653.
8. Lykke M, Hother AL, Hansen CF, *et al.* (2013) Malnutrition induces gut atrophy and increases hepatic fat infiltration: studies in a pig model of childhood malnutrition. *Am J Transl Res* **5**, 543–554.
9. Miyazaki A, Kandasamy S, Michael H, *et al.* (2018) Protein deficiency reduces efficacy of oral attenuated human rotavirus vaccine in a human infant fecal microbiota transplanted gnotobiotic pig model. *Vaccine* **36**, 6270–6281.
10. Núñez IN, Galdeano CM, Carmuega E, *et al.* (2013) Effect of a probiotic fermented milk on the thymus in Balb/c mice under non-severe protein-energy malnutrition. *Br J Nutr* **110**, 500–508.
11. Teodósio NR, Lago ES, Romani SA, *et al.* (1990) A regional basic diet from northeast Brazil as a dietary model of experimental malnutrition. *Arch Latinoam Nutr* **40**, 533–547.
12. Ueno PM, Oría RB, Maier EA, *et al.* (2011) Alanine-glutamine promotes intestinal epithelial cell homeostasis *in vitro* and in a murine model of weanling undernutrition. *AJP Gastrointest Liver Physiol* **301**, G612–G622.
13. Sampaio IC, Medeiros PHQS, Rodrigues FAP, *et al.* (2016) Impact of acute undernutrition on growth, ileal morphology and nutrient transport in a murine model. *Braz J Med Biol Res* **49**, 1–10.
14. Brown EM, Wlodarska M, Willing BP, *et al.* (2015) Diet and specific microbial exposure trigger features of environmental enteropathy in a novel murine model. *Nat Commun* **6**, 1–16.
15. Bolick DT, Roche JK, Hontecillas R, *et al.* (2013) Enteropathogenic *Escherichia coli* strain in a novel weaned mouse model: exacerbation by malnutrition, biofilm as a virulence factor and treatment by nitazoxanide. *J Med Microbiol* **62**, 896–905.
16. De Queiroz CA, Fonseca SGC, Frota PB, *et al.* (2014) Zinc treatment ameliorates diarrhea and intestinal inflammation in undernourished rats. *BMC Gastroenterol* **14**, 1–14.
17. Paixão ADO, Aléssio MLM, Martins JPC, *et al.* (2006) Regional Brazilian diet-induced pre-natal malnutrition in rats is correlated with the proliferation of cultured vascular smooth muscle cells. *Nutr Metab Cardiovasc Dis* **15**, 302–309.
18. Barros KMFT, Manhães-De-Castro R, Lopes-De-Souza S, *et al.* (2006) A regional model (Northeastern Brazil) of induced malnutrition delays ontogeny of reflexes and locomotor activity in rats. *Nutr Neurosci* **9**, 99–104.
19. Turner JR (2009) Intestinal mucosal barrier function in health and disease. *Nat Rev Immunol* **9**, 799–809.
20. Cahill GF (2006) Fuel metabolism in starvation. *Annu Rev Nutr* **26**, 1–22.
21. Radtke F & Clevers H (2005) Self-Renewal and cancer of the gut: two sides of a coin. *Sci* **307**, 1904–1909.
22. Carle MS (2010) Validation of Bioimpedance Spectroscopy by Assessing. PhD Thesis, University of Alabama. Validity of Bioimpedance Spectroscopy in the Assessment of Total Body Water and Body Composition in Wrestlers and Untrained Subjects - PubMed. nih.gov (accessed April 2021).
23. Barboza MS, Silva TMJ, Guerrant RL, *et al.* (1999) Measurement of intestinal permeability using mannitol and lactulose in children with diarrheal diseases. *Braz J Med Biol Res* **32**, 1499–1504.
24. Livak KJ & Schmittgen TD (2001) Analysis of relative gene expression data using real-time quantitative PCR and the $2^{-\Delta\Delta C(T)}$ Method. *Method* **25**, 402–408.
25. Agosti M, Tandoi F, Morlacchi L, *et al.* (2017) Nutritional and metabolic programming during the first thousand days of life. *La Pediatr Med e Chir* **39**, 57–61.
26. Weage K, Maier EA, Guedes MM, *et al.* (2013) Undernutrition by a regional basic diet increases serum interferon- γ levels and enhances tolerance to oral lipopolysaccharide in weanling mice. *AGA* **1**, S316.
27. Almeida MFL, Yamasaki EN, Silveira ACD, *et al.* (2001) The GABAergic and cholinergic systems in the retina are differentially affected by postnatal malnutrition during the suckling period. *Nutr Neurosci* **4**, 223–238.
28. Soeters P, Bozzetti F, Cynober L, *et al.* (2016) Defining malnutrition: a plea to rethink. *Clin Nutr* **36**, 896–901.
29. Butsch WS & Heimburger DC (2008) Malnutrition and disease outcomes. *Gastroenterology, nutrition and gastrointestinal disease*. In *Nutrition and Gastrointestinal Disease* [MH DeLEGGE, editor]. Totowa, NJ: Human Press.
30. Benabe JE & Martinez-Maldonado M (1998) The impact of malnutrition on kidney function. *Miner Electrolyte Metab* **24**, 20–26.
31. Grover Z & Ee LC (2009) Protein energy malnutrition. *Pediatr Clin N Am* **56**, 1055–1068.
32. Gartner A, Berger J, Simondon KB, *et al.* (2003) Change in body water distribution index in infants who become stunted between 4 and 18 months of age. *Eur J Clin Nutr* **57**, 1097–1106.
33. Earthman WH, Mathie JR, Reid PM, *et al.* (2000) Body cell mass change in HIV infection A comparison of bioimpedance methods for detection of A comparison of bioimpedance methods for detection of body cell mass change in HIV infection. *J Appl Physiol* **88**, 944–956.
34. Cheek DB, Hill DE, Cordano A, *et al.* (1970) Malnutrition in infancy: changes in muscle and adipose tissue before and after rehabilitation. *Pediatr Res* **4**, 135–144.
35. Ferraris RP & Carey HV (2000) Intestinal transport during fasting and malnutrition. *Annu Rev Nutr* **20**, 195–219.
36. Edelblum KL, Yan F, Yamaoka T, *et al.* (2005) Regulation of apoptosis during homeostasis and disease in the intestinal epithelium. *Inflamm Bowel Dis* **12**, 413–424.
37. Lima AAM, Brito LFB, Ribeiro HB, *et al.* (2005) Intestinal barrier function and weight gain in malnourished children taking glutamine supplemented enteral formula. *J Pediatr Gastroenterol Nutr* **40**, 28–35.
38. Lima NL, Soares AM, Mota RMS, *et al.* (2007). Wasting and intestinal barrier function in children taking alanine-glutamine-supplemented enteral formula. *J Pediatr Gastroenterol Nutr* **44**, 365–374.
39. Krugliak P, Hollander D, Schlaepfer CC, *et al.* (1994) Mechanisms and sites of mannitol permeability of small and large intestine in the rat. *Dig Dis Sci* **39**, 796–801.
40. Hossain MI, Haque R, Mondal D, *et al.* (2016) Undernutrition, vitamin A and iron deficiency are associated with impaired intestinal mucosal permeability in young Bangladeshi children assessed by lactulose/mannitol test. *PLOS ONE* **11**, 1–10.

41. Lee GO, Kosek P, Lima AAM, *et al.* (2014) Lactulose: mannitol diagnostic test by HPLC and LC-MSMS platforms: considerations for field studies of intestinal barrier function and environmental enteropathy. *J Pediatr Gastroenterol Nutr* **59**, 544–550.
42. Lima AA, Leite Alvaro M, Di Moura A, *et al.* (2017) Determinant variables, enteric pathogen burden, gut function, and immune-related inflammatory biomarkers associated with childhood malnutrition. *Pediatr Infect Dis J* **36**, 1177–1185.
43. Lima AAM, Oria RB, Soares AM, *et al.* (2014) Geography, population, demography, socioeconomic, anthropometry, and environmental status in the MAL-ED cohort and case-control study sites in Fortaleza, Ceará, Brazil. *Clin Infect Dis* **59**, S287–S294.
44. Jacobi SK, Moeser AJ, Blikslager AT, *et al.* (2013) Acute effects of rotavirus and malnutrition on intestinal barrier function in neonatal piglets. *World J Gastroenterol* **19**, 5094–5102.
45. Suzuki T (2013) Regulation of intestinal epithelial permeability by tight junctions. *Cell Mol Life Sci* **70**, 631–659.
46. Tamura A, Hayashi H, Imasato M, *et al.* (2011) Loss of claudin-15, but not claudin-2, causes Na⁺ deficiency and glucose malabsorption in mouse small intestine. *Gastroenterology* **140**, 913–923.
47. Wada M, Tamura A, Takahashi N, *et al.* (2013) Loss of claudins 2 and 15 from mice causes defects in paracellular Na⁺ flow and nutrient transport in gut and leads to death from malnutrition. *Gastroenterology* **144**, 369–380.
48. McCarthy KM, Skare IB, Stankewich MC, *et al.* (1996) Occludin is a functional component of the tight junction. *J Cell Sci* **109**, 2287–2298.
49. Furuse M, Hirase T, Itoh M, *et al.* (1993) Occludin: a novel integral membrane protein localizing at tight junctions. *J Cell Biol* **123**, 1777–1788.
50. Furuse M, Hata M, Furuse K, *et al.* (2002) Claudin-based tight junctions are crucial for the mammalian epidermal barrier: a lesson from claudin-1-deficient mice. *J Cell Biol* **156**, 1099–1111.
51. Anderson JM & Itallie CMV (2009) Physiology and function of the tight junction. *Cold Spring Harb Perspect Biol* **1**, 1–16.
52. Li N, Lassman BJ, Liu Z, *et al.* (2004) Effects of protein deprivation on growth and small intestine morphology are not improved by glutamine or glutamate in gastrostomy-fed rat pups. *J Pediatr Gastroenterol Nutr* **39**, 28–33.
53. Boudry G, David ES, Douard V, *et al.* (2010) Role of intestinal transporters in neonatal nutrition: carbohydrates, proteins, lipids, minerals, and vitamins. *J Pediatr Gastroenterol Nutr* **51**, 380–401.
54. Freeman TC, Wood IS, Sirinathsinghji DJS, *et al.* (1993) The expression of the Na⁺/glucose cotransporter (SGLT1) gene in lamb small intestine during postnatal development. *BBA* **1146**, 203–212.
55. Ferraris RP (2001) Dietary and developmental regulation of intestinal sugar transport. *Biochem J* **360**, 265–276.
56. Gilbert ER, Wong EA & Webb KE (2008) Peptide absorption and utilization: implications for animal nutrition and health. *J Anim Sci* **86**, 2135–2155.